Journal of Power Sources 186 (2009) 238–243

Contents lists available at ScienceDirect

Journal of Power Sources

journal homepage: www.elsevier.com/locate/jpowsour

Ag current collector for honeycomb solid oxide fuel cells using $LaGaO_3$-based oxide electrolyte

Hao Zhong[a], Hiroshige Matsumoto[a,b], Tatsumi Ishihara[a,b,*], Akira Toriyama[c]

[a] Department of Applied Chemistry, Faculty of Engineering, Kyushu University, Motooka 744, Nishi-Ku, Fukuoka 819-0395, Japan
[b] Center for Future Chemistry, Kyushu University, Motooka 744, Nishi-Ku, Fukuoka 819-0395, Japan
[c] Thinktank Phoenix Co. Ltd., Nakano-ku, Tokyo, Japan

ARTICLE INFO

Article history:
Received 3 August 2008
Received in revised form 13 October 2008
Accepted 15 October 2008
Available online 5 November 2008

Keywords:
Honeycomb SOFC
Anode
Current collector
$LaGaO_3$ electrolyte

ABSTRACT

Honeycomb type solid oxide fuel cell (SOFC) using a Ag mesh as a current collector and $La_{0.9}Sr_{0.1}Ga_{0.8}Mg_{0.2}O_3$ (LSGM) as an electrolyte was studied for reducing production cost. When an Ag mesh was used as a current collector, the power density of the cell became lower than that of a cell using a Pt mesh due to the relatively worse contact caused by the lower calcination temperature, particularly in the case of the anode. The preparation method and the electrode structure were investigated for the purpose of increasing the power density of the cell using the Ag current collector. It was found that an interlayer of Ni–$Sm_{0.2}Ce_{0.8}O_{1.9}$ (1:9) between the NiFe–LSGM cermet anode and the LSGM electrolyte was effective for decreasing the pre-calcination temperature for anode fabrication. Much higher power densities of 300 mW cm^{-2} and 140 mW cm^{-2} at 1073 K and 973 K, respectively, were achieved by inserting an interlayer. These results for the power density of the cell using the Ag mesh current collector after the optimization of the electrode structure and the preparation procedure are close to those of the cell using the Pt mesh current collector cell presented in our previous work.

1. Introduction

Solid oxide fuel cells (SOFCs) constitute a type of advanced technology for the efficient generation of electricity [1–3]. So far, two types of SOFC structures, tubular and planar, have been studied [1–3]. Tubular SOFCs have certain advantages, such as technical simplicity and reliability, as well as disadvantages such as low power density and high manufacturing cost. In contrast, planar-type SOFCs feature a high power density and low manufacturing cost, however, disadvantages of difficulty in a gas sealing and slightly larger degradation in power density. The "ideal SOFC" combines the features of both tubular and planar type SOFCs. In this regard, the so-called honeycomb type fuel cell, which employs a new and unique SOFC concept, has being recently attracting much interest [4–8]. The honeycomb SOFCs can be described as 'a condensed collection of small tubes', and has advantages such as high volumetric power density, high mechanical strength, and superior thermal management, i.e. heat exchange property. However, the difficulties associated with the fabrication of the electrodes in the narrow channels and interconnections of the cells are drawbacks which still need to be overcome. The first honeycomb SOFC, which is used ZrO_2 electrolyte, was successfully produced by the ABB group [4], and they reported a power density of 0.1 W cm^{-2} at 1273 K [4]. Although a stainless interconnector was successfully applied in this cell, its operating temperature is too high for using a stainless interconnector, while the power density is not high. Therefore, decrease in the operating temperature, in other words, an improvement in the power density is required in order to be able to get the advantages of honeycomb cells, particularly their high volumetric power density.

We previously reported [9–11] that a $La_{0.9}Sr_{0.1}Ga_{0.8}Mg_{0.2}O_3$ (LSGM)-based honeycomb cell exhibits a much higher power density than that of a ZrO_2-based one at the same operation temperatures because of the superior oxide ion conductivity of LSGM. A Pt current collector was always used in the previous cell studied, and the anode oxide was applied on the Pt mesh as a current collector, in which a reasonably high power density was achieved (0.5 W cm^{-2}, 1.9 W cm^{-3} at 1073 K) in our previous study. However, considering the commercial production of this LSGM-based honeycomb SOFC, reduction of the cost is required since a large amount of expensive Pt mesh is used for the current collector. In fact, nickel felt, which is cheap metal, is popularly used for a current collector in the developing SOFCs. Accordingly, the Pt mesh used in the configuration of the present cell was replaced with a mesh

* Corresponding author at: Department of Applied Chemistry, Faculty of Engineering, Kyushu University, Motooka 744, Nishi-Ku, Fukuoka 819-0395, Japan.
Fax: +81 92 802 2868.
E-mail address: ishihara@cstf.kyushu-u.ac.jp (T. Ishihara).

0378-7753/$ – see front matter © 2008 Elsevier B.V. All rights reserved.
doi:10.1016/j.jpowsour.2008.10.083

made of a cheaper metal, in this case Ag. Since the cermet anode is pre-calcined on the honeycomb at 1373 K in order to achieve good contact, the greatest difficulty associated with using the Ag current collector is the low melting point of Ag. Therefore, it is necessary to decrease the electrode fabrication temperature, in other words, the calcination temperature of the cermet anode needs to be lower than 1173 K. However, by decreasing the calcination temperature for the preparation of the Ni-based cermet anode, it is anticipated that the contact resistance will increase, resulting in the decreased power density. This problem can be solved in two ways. The first involves the calcination of the Ag mesh after the attachment of the cermet anode on the honeycomb cell at a reasonably high temperature. However, this method entails a decrease in the current collecting efficiency due to an insufficient contact. The second way involves simply lowering of the anode pre-calcination temperature. However, this has an adverse effect on both the contact and the mechanical strength of the anode. In this study, influence of an interlayer between the anode and the LSGM electrolyte was studied with regard to improving the contact when using the Ag mesh current collector. Furthermore, the power generation properties of a LSGM honeycomb cell with thinner walls and the Ag mesh current collector was investigated by using a single-wall cell with the structure reported in our previous paper [9].

2. Experimental

A LSGM honeycomb cell was prepared by using a LSGM honeycomb electrolyte prepared by one kind of a slip-casting method developed by Kikusui Chemical Industry Co. Ltd. and using NiFe91–LSGM (90:10) (NiFe91, 9:1 in metal weight ratio; NiFe91–LSGM = 90:10 in weight ratio) for the anode and $Sm_{0.5}Sr_{0.5}CoO_3$ (SSC55) for the cathode, which was prepared with the solid-state reaction method [12]. The honeycomb cell used a self-supported electrolyte, and had the following dimensions: 19 mm width, 20 mm height, and 1 mm or 0.5 mm wall thickness. A photograph of the cell used in this study is shown in Fig. 1.

A Ni–$Ce_{0.8}Sm_{0.2}O_{1.9}$ (SDC) (1:9 in weight ratio) interlayer was inserted at the anode/honeycomb electrolyte interface in order to increase its compatibility with the anode electrode as well as to prevent a reaction between the Ni-based anode and the LSGM electrolyte. NiO and SDC powders were first dispersed into toluene with polyvinyl butyral for the preparation of slurry, which was subsequently coated on the LSGM honeycomb and then sintered at 1473 K for 6 h.

For the preparation of the electrode slurry, the powders were first dispersed into toluene by using polyvinyl butyral. As a default preparation process, the anode and the cathode slurry were coated on their respective sides of the interior LSGM honeycomb channel, and were subsequently sintered at 1373 K (for the anode) and 1173 K (for the cathode) for 1 h, unless otherwise noted. In the case of the cell using a Ni–SDC interlayer, the anode and the cathode were calcined simultaneously at 1173 K for 1 h.

A commercial Ag mesh (Tanaka Kikinzoku Co. Ltd., 60 mesh, 0.1 mm line radius) was used as a current collector. In order to achieve better current collecting efficiency, a thinner Ag mesh was produced by pressing the commercial mesh, which is shown in Fig. 2(b). The Ag mesh was fixed on top of the NiFe–LSGM anode or the SSC-55 cathode with Pt paste. Ag paste could be used instead of Pt paste, however, in this study, because the amount of Pt is not large and also a reasonable high strength is obtained, Pt past was used for fixing the Ag mesh. Furthermore, a schematic representation of the electrode structure with the interlayer in this study is shown in Fig. 2(c).

The honeycomb cell thus prepared was set into a stainless steel gas manifold, which is reported previously [11] and humidified hydrogen (3 vol% H_2O, 150 mL min^{-1}) and oxygen (150 mL min^{-1}) were used as fuel and oxidant, respectively. It is also noted that the fuel utilization is always lower than 20% in this study. The power generation properties were measured with the four-probe method, where a galvanostat/potentiostat (Hokuto, HA301) was used as electronic load. The internal resistance was measured using the current interruption method.

3. Results and discussion

Since the commercially available Ag mesh (Fig. 2(a)) was too difficult to use as a suitable current collector as received in the honeycomb SOFC due to its large line radius and mesh size, we pressed it into a much thinner mesh, which is shown in Fig. 2(b) in order to achieve an acceptable handling performance for the cell fabrication. Fig. 3 shows the *I–V* and *I–P* curves at 1073 K of the honeycomb fuel cells with Ag and Pt mesh current collectors. The maximum power density of the cell using the Ag mesh current collector was ca. 250 mW cm^{-2}, which is much lower than that of the cell using

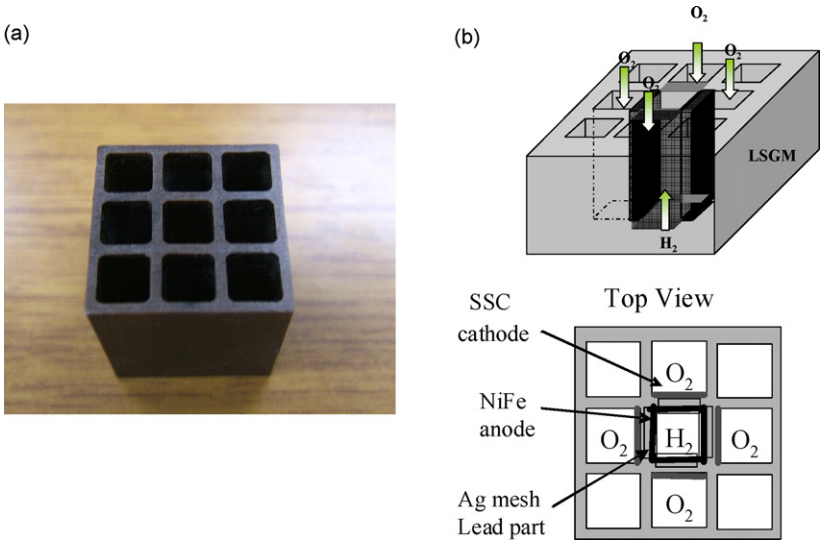

Fig. 1. Photograph of the LSGM honeycomb used in this experiment (1.0 mm thick wall). (a) Photograph of the LSGM honeycomb used, (b) scheme of the single channel cell. (Figure is one channel (4-wall used) type cell and single wall was used in large part of this study.)

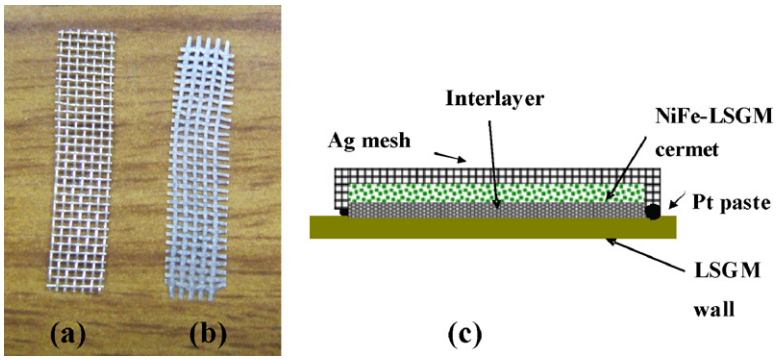

Fig. 2. Photographs of the Ag mesh (a) in its original state and (b) after it has been pressed. (c) A schematic view of the electrode with the Ag mesh current collector with interlayer.

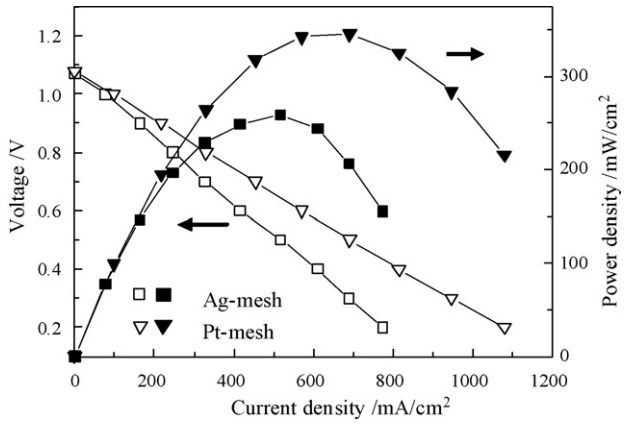

Fig. 3. *I–V* and *I–P* curves corresponding to the following conditions: H_2 (3% H_2O), Ag mesh, NiFe91–LSGM/LSGM honeycomb (1.0 mm)/SSC, Ag mesh, O_2 cell at 1073 K.

the Pt mesh current collector, even though the mesh was pressed thin for improved handling.

Fig. 4 shows the internal resistances of the cell with the Ag mesh and that with the Pt mesh at 1073 K. It is clear that both the IR loss and the overpotential increased by using the Ag mesh instead of the Pt mesh, and the main reason for the decrease in power density can be attributed to the increase in IR loss. In our previous report, where the Pt mesh was used as a current collector, the mesh was

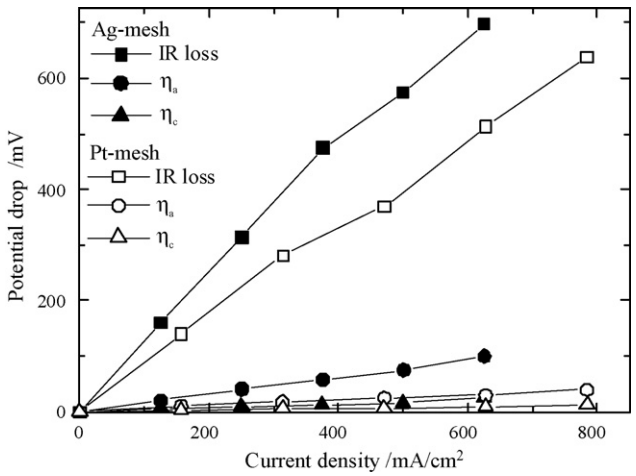

Fig. 4. Plots of the IR loss and the overpotential of the cells with a Ag mesh, NiFe91–LSGM/LSGM honeycomb (1.0 mm)/SSC, Ag mesh honeycomb at 1073 K. IR: IR loss, η_{an}: anodic overpotential, η_{ca}: cathodic overpotential.

attached on a LSGM honeycomb before coating the anode slurry with Pt paste, which ensured good contact between the Pt mesh and the anode powder. In contrast, when using the Ag mesh as the current collector, the mesh should be attached to the LSGM honeycomb after the calcination of the anode because of the relatively low melting point of Ag. The reversed fabrication order decreases the current collecting efficiency, which entails the increase in IR loss. Therefore, the lower power generating performance of the cell with the Ag mesh (Fig. 3) can be attributed to the large contact resistance between the electrode powder (both anode and cathode) and the Ag mesh current collector. The following points are also considered as possible reasons for the large IR loss: delamination of the electrodes, particularly the anode, caused by mismatching thermal expansion coefficients, insufficient net growth of the cermet powder due to the low calcination temperature, and a reaction between the NiFe–LSGM cermet electrode with the LSGM electrolyte due to the fact that the IR loss between the anode and the reference electrode is much larger than that between the reference electrode and the cathode. It should also be noted that the anodic overpotential of the cell using the Ag mesh current collector was also larger than that of the Pt mesh cell. Therefore, the increased IR loss and anodic overpotential were studied in detail.

One reason for the considerable IR loss can be attributed to the reaction layer formed between the NiFe anode and the LSGM electrolyte since the anode was directly coated onto the LSGM electrolyte and calcined at 1373 K in the case of the Ag mesh cell shown in Fig. 3. In our previous work, the insertion of a SDC layer between the Ni-based anode and the LSGM electrolyte proved to be effective for preventing a reaction between the Ni electrode and the LSGM electrolyte [13]. Furthermore, influence of the interlayer, which is shown in Fig. 2(c), on the power generation properties of the cell were studied with regard to improving the power density. Fig. 5 shows the influence of the interlayer on the power density of the cell using the Ag mesh current collector. It is clear that the power density is greatly improved (from 250 mW cm^{-2} to 300 mW cm^{-2}) by the insertion of a LSGM or Ni–SDC interlayer, albeit it still lower than that of the cell using the Pt mesh. Although the power density of both cells is almost the same, it is slightly higher for the cell with the LSGM interlayer than that for the one with Ni–SDC interlayer. However, because of the decreased anodic overpotential, which is discussed later, we adopted Ni–SDC for the interlayer between the NiFe–SDC anode and the electrolyte. Since the IR loss was greatly reduced by the Ni–SDC interlayer, it seems that the improved power density can be attributed to the suppression of the formation of a secondary phase between the NiFe anode and the LSGM electrolyte (see details in Fig. 7). Since better current collecting efficiency can be achieved for the cell by increasing the post-calcination temperature after coating, influence of the calcination temperature of the

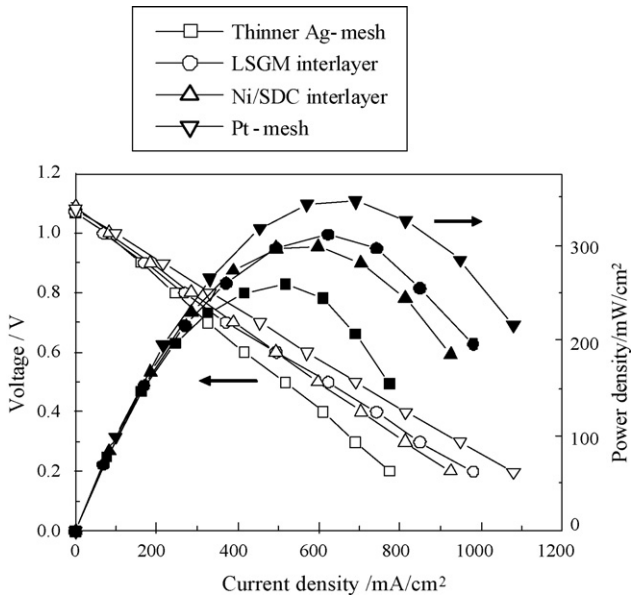

Fig. 5. Influence of the interlayer on the power density of the honeycomb cell using the Ag mesh current collector at 1073 K.

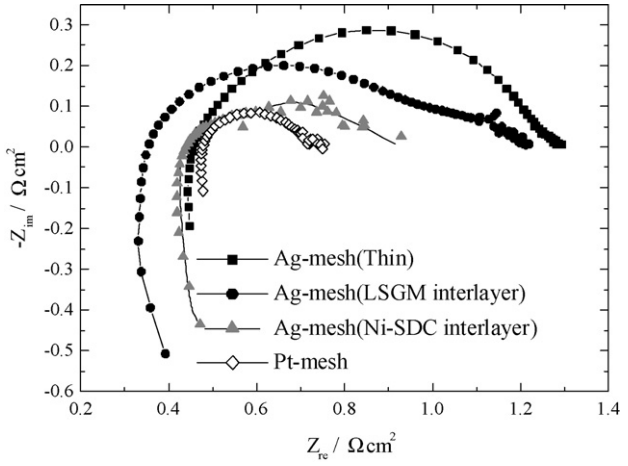

Fig. 6. Complex impedance spectra of the anode of the cell with an interlayer under open circuit conditions at 1073 K.

Ni–SDC and LSGM interlayer on the power density was studied in order to achieve an improved current collecting performance.

Fig. 6 shows the influence of the interlayer on the complex impedance spectra for the anode reaction. Compared with that of the Pt mesh, a much larger semicircle was observed for the Ag mesh. Therefore, the decreased power density cannot be explained with the increased IR loss, but rather with the larger anodic overpotential, which is in good agreement with the results obtained with the current interruption method (Fig. 4). On the other hand, the insertion of Ni–SDC is effective for decreasing the size of the anodic semicircle, which suggests that the Ni–SDC interlayer is effective

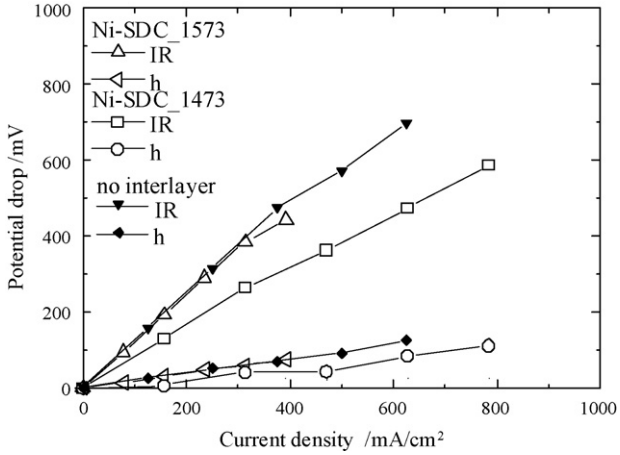

Fig. 7. Details of the potential drop of the cell at 1073 K with a Ni–SDC interlayer prepared at 1473 K and 1573 K.

for improving the anodic reaction. In contrast, in the case of a LSGM interlayer, the resistance of the interface of the semicircle at higher frequencies decreased, which suggests that the contact resistance can be greatly improved by the application of a LSGM interlayer. However, the size of the anodic impedance semicircles is almost the same as that of the Ag mesh. Therefore, the improvement in power density by the LSGM interlayer is explained mainly by the decreased contact resistance of the anode. Accordingly, taking into account the decreased anodic overpotential, we studied the optimization of the Ni–SDC interlayer preparation procedure in detail. At present, details reason for improving activity of NiFe–LSGM anode by insertion of Ni–SDC interlayer is not clear, however, it is reported that CeO_2 is active to oxidation reaction [14,15] and so, electrochemical oxidation activity of anode is improved by catalytic effects of SDC interlayer. Another more reasonable reason seems to be expanded electrode area by preventing a delamination of NiFe–LSGM cermet anode and preventing the reaction between electrode and electrolyte. Because of the low melting point of Ag, NiFe–LSGM anode is easily delaminated because of the low calcination temperature (<1173 K) and if the anode is partially delaminated condition, then the anodic overpotential would be enlarged because of a concentrated current line.

Table 1 summarizes the influence of the calcination temperature for the Ni–SDC interlayer on the open circuit potential, the maximum power density (MPD), and the internal resistance of the cells in which an interlayer was used. It is clear that the maximum power density increased together with the calcination temperature, reaching its maximum at a calcination temperature of 1473 K. Furthermore, Fig. 7 shows the details of the potential drop for cells using a Ni–SDC interlayer calcined at 1473 K and 1573 K and a cell without a Ni–SDC interlayer. As shown in Fig. 7, the IR loss of the cell was greatly reduced by the insertion of the Ni–SDC interlayer, reaching its minimum when the Ni–SDC interlayer was calcined at 1473 K. Therefore, the improvement of the power density due to the increase in the calcination temperature of Ni–SDC can be explained with the improved contact between Ni–SDC and the LSGM elec-

Table 1
Influence of the Ni–SDC interlayer on the power generating properties of the cell with a Ag mesh current collector at 1073 K.

Cell	Interlayer calcination temperature (K)	Anode calcination temperature (K)	Open circuit voltage (V)	Maximum power density (mW cm^{-2})
Thin Ag mesh	–	1373	1.07	250
Ni–SDC (1:9) interlayer	1373	1173	0.95	60
Ni–SDC (1:9) interlayer	1473	1173	1.09	300
Ni–SDC (1:9) interlayer	1573	1173	1.10	205

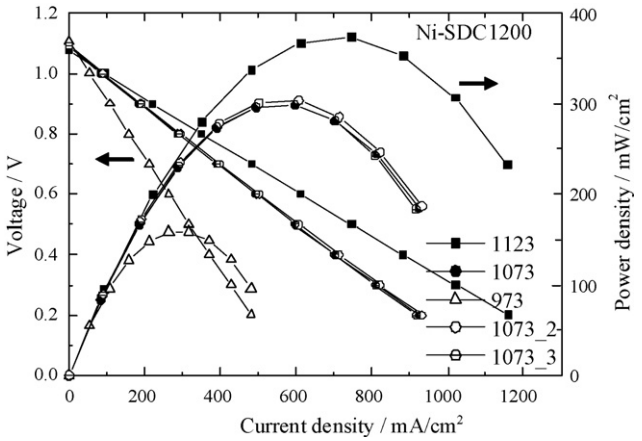

Fig. 8. Temperature dependence of the optimized cell with the Ag current collector. Ag-mesh, NiFe91–LSGM/Ni–SDC/LSGM honeycomb (1.0 mm)/SSC, Ag-mesh cell. The last digit in 800, 800_2, and 800_3 indicates the number of the thermal cycle.

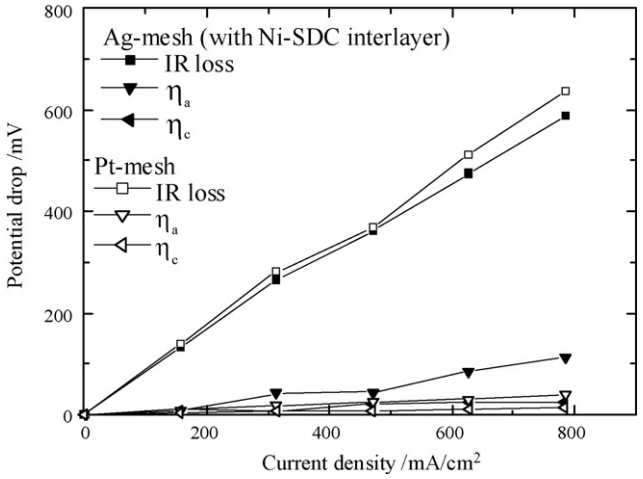

Fig. 9. Details of the internal resistance at 1073 K for the cell with the Ag mesh and that with the Pt mesh Ag mesh: Ag-mesh, NiFe91–LSGM/Ni–SDC/LSGM honeycomb (1.0 mm)/SSC, Ag mesh. Pt mesh: Pt-mesh, NiFe91–LSGM/LSGM/SSC, Pt mesh.

trolyte. It should also be noted that the IR loss increased when the calcination of the Ni–SDC interlayer was performed at excessively high temperatures (Fig. 7). The highest power density was achieved at the optimum calcination temperature of 1473 K for the Ni–SDC interlayer. It was also found that the anodic overpotential was reduced due to the insertion of the Ni–SDC interlayer, which indicates that the interlayer is effective for improving the anodic reactivity. Furthermore, the value of the thermal expansion coefficient of the Ni–SDC interlayer is intermediate between those of the NiFe–LSGM anode and the LSGM electrolyte, which also indicates that the compatibility of the NiFe–LSGM cermet anode with the LSGM electrolyte can be improved through the suppression of the anode delamination associated with the insertion of a Ni–SDC interlayer. Due to the high activity of SDC for anodic reactions, the surface activity with respect to the electrochemical oxidation of H_2 can also be improved. In any case, it is clear that the optimum calcination temperature for Ni–SDC interlayer is 1473 K.

Fig. 8 shows the temperature dependence of the cell obtained when the Ni–SDC interlayer was calcined at 1473 K, followed by the preparation of the Ni–LSGM cermet anode. The open circuit voltage (OCV) of the cell is approximately 1.08 V at all measured temperatures, showing only a slight increase when the temperature decreased. The observed OCV was close to that of the theoretical OCV, suggesting that the gas sealing of the cell is sufficiently high. The maximum power densities were about 300 mW cm^{-2} and 140 mW cm^{-2} at 1073 K and 1023 K, respectively. The thermal stability of the cell was also studied, and the results are shown in Fig. 8. Evidently, the thermal cycling stability of the honeycomb cell after the optimization was adequate. The term 'thermal cycling' indicates that the cell cools to room temperature and then heats up to the operating temperature, where both the cooling and the heating rate are 100 K h^{-1}, respectively. Fig. 8 also shows the power generation properties of the cell after the 3rd thermal cycle, where it is clear that there is no degradation. In comparison to the cell with the Pt mesh, the cell containing the Ag mesh and the Ni–SDC interlayer exhibits an improved stability against thermal cycling treatment. More specifically, the use of a suitable interlayer is effective for improving the compatibility of the anode by matching the thermal expansion coefficient and preventing unfavorable reactions. As a result, it is concluded that the much cheaper Ag mesh can be used as a current collector in the honeycomb SOFCs, although the power density of such cells is still lower than that of the cell using the Pt mesh.

Fig. 9 shows a comparison of the internal resistances at 1073 K of the optimized cell with the Ag mesh current collector and that of a cell with the Pt mesh. It was found that the cell using the Ag mesh as a current collector has almost the same IR loss as compared with that of the Pt mesh cell, although its anodic overpotential is slightly larger. Therefore, although it is likely that the material problems of the current collector can be solved by optimizing the cell structure and the preparation conditions, the anodic overpotential is expected to increase due to the different in the anode calcination temperatures for the two types of cells.

In order to identify the reasons for the increase in the anodic overpotential, the anodic impedance semicircles of the cell with the Ag mesh after optimization were compared with those of the Pt mesh cell in details (Fig. 6). As discussed previously, the observed semicircles of both cells consist of several smaller semicircles, which can be roughly assigned to the activation and diffusion overpotential at higher and lower frequencies. Comparing the impedance plots of the Pt mesh cell, it is evident that the lower frequency semicircle is much larger, and thus the observed larger anodic overpotential on Ag mesh cell can be attributed to its larger diffusion overpotential. This can be explained with the increase in the thickness of the anode electrode caused by the insertion of a Ni–SDC interlayer. Therefore, by controlling the thickness of the Ni–SDC interlayer, the anodic overpotential can be reduced in the case of Ag mesh cells. Influence of the Ni–SDC interlayer on the

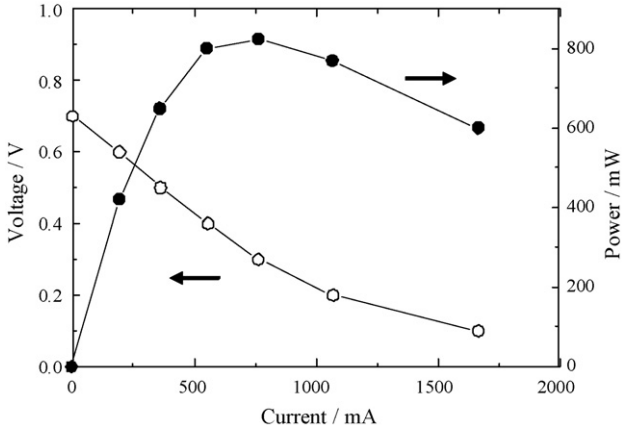

Fig. 10. Power generation curves at 1073 K of the 4-wall LSGM honeycomb cell with 0.5 mm wall thickness using a Ag mesh as current collector.

power density of the cell is currently under investigation, and the results will be reported elsewhere.

Finally, power generation measurements for the 4-wall honeycomb cell with 0.5 mm wall thickness were carried out after the successful power generation measurements for the single-wall honeycomb cell with 1.0 mm wall thickness and Ag mesh current collector. The *I–P* and *I–V* curves of the 4-wall honeycomb cell with 0.5 mm wall thickness at 1073 K are shown in Fig. 10. The observed OCV is only 0.7 V, which is much lower than that of the theoretical one (1.10 V), indicating that the gas sealing in this case is not sufficient. However, even under such gas leakage conditions, the output power was about 800 mW, which corresponds to an area specific power density of 250 mW cm^{-2}, and a volumetric power density of 0.5 kW L^{-1} when one and 4 channels are used as fuel and oxidant channels, respectively. As a result, it can be said that the honeycomb cell structure provides sufficiently high volumetric power density in comparison to the conventional cell design.

4. Conclusion

A LSGM honeycomb SOFC in which the Ag mesh was used as a current collector was successfully fabricated and operated in this study. Sufficiently high power density was achieved for this cell by using a thin Ag mesh directly connected to the anode, and further improvement was achieved by the addition of a Ni–SDC interlayer calcined at 1473 K. The effectiveness of the interlayer is attributable to the suppression of the reaction between the anode and the electrolyte as well as to the decreased anode calcination temperature. Therefore, Ni–SDC interlayer could be used not only for honeycomb type but also other type SOFCs like tubular or planer type when $LaGaO_3$-based oxide is used for the electrolyte. The highest MPD values were about 300 mW cm^{-2} and 140 mW cm^{-2} at 1073 K and 973 K, respectively, which are close to the power density of the previously reported cell using the Pt mesh current collector. These results indicate that it is possible to replace the Pt mesh with the Ag mesh and still obtain acceptable results. This study revealed that a reasonably high power density can be achieved by using the Ag current collector and a LSGM honeycomb structure.

References

[1] T. Ishihara, M. Honda, T. Shibayama, H. Minami, H. Nishiguchi, Y. Takita, J. Electrochem. Soc. 145 (1998) 3177.
[2] T. Ishihara, H. Matsuda, Y. Takita, J. Am. Chem. Soc. 116 (1994) 3801.
[3] T. Ishihara, H. Matsuda, Y. Takita, Solid State Ionics 79 (1995) 147.
[4] M. Wetzko, A. Belzner, F.J. Rohr, F. Harbach, J. Power Sources 83 (1999) 148.
[5] F.J. Rohr, A. Reich, N. Pfeifer, European Patent EP 0,503,526 (1992).
[6] S. Zha, Y. Zhang, M. Liu, Solid State Ionics 176 (2004) 25.
[7] M. Shinagawa, T. Ishihara, A. Kawakami, H. Nishiguchi, Y. Takita, Meet. Abstr.: Electrochem. Soc. 501 (2006) 1140.
[8] T. Yamaguchi, S. Shimizu, T. Suzuki, Y. Fujishiro, M. Awano, Electrochem. Solid-State Lett. 11 (2008) B117–121.
[9] H. Zhong, H. Matsumoto, T. Ishihara, A. Toriyama, Chem. Lett. (2007) 846.
[10] H. Zhong, H. Matsumoto, T. Ishihara, A. Toriyama, Mater. Sci. Forum 544–545 (2007) 969.
[11] H. Zhong, H. Matsumoto, T. Ishihara, A. Toriyama, ECS Trans., SOFC X. PV 7 (1) (2007) 669.
[12] T. Ishihara, M. Honda, T. Shibayama, H. Nishiguchi, Y. Takita, J. Electrochem. Soc. 145 (1998) 3177.
[13] J. Akikusa, T. Yamada, T. Kotani, N. Murakami, T. Akbay, A. Hasegawa, M. Yamada, N. Komada, S. Nakamura, N. Chitose, K. Hirata, S. Sato, T. Miyazawa, M. Shibata, K. Hosoi, F. Nishiwaki, T. Inagaki, J. Kano, S. Ujiie, T. Matsunami, H. Nakajima, J. Nishi, T. Sasaki, H. Yoshida, K. Hashino, M. Kawano, S. Yamasaki, Y. Takita, T. Ishihara, J. Electrochem. Soc. 153 (2006) A.589–A594.
[14] T. Masui, K. Minami, K. Koyabu, N. Imanaka, Catal. Today 117 (2006) 187.
[15] S. Zhao, R.J. Gorte, Appl. Catal. A 277 (2004) 129.